

## A wide-range multi-channel Air Ion Spectrometer

Aadu Mirme<sup>1)</sup>, Eduard Tamm<sup>1)</sup>, Genrik Mordas<sup>2)</sup>, Marko Vana<sup>1)2)</sup>, Janek Uin<sup>1)</sup>, Sander Mirme<sup>1)</sup>, Toomas Bernotas<sup>1)</sup>, Lauri Laakso<sup>2)</sup>, Anne Hirsikko<sup>2)</sup> and Markku Kulmala<sup>2)</sup>

<sup>1)</sup> Department of Environmental Physics, University of Tartu, 18 Ülikooli St., 50090 Tartu, Estonia

<sup>2)</sup> Division of Atmospheric Sciences, Department of Physical Sciences, P.O. Box 64, FI-00014 University of Helsinki, Finland

Received 16 Oct. 2006, accepted 19 Mar. 2007 (Editor in charge of this article: Veli-Matti Kerminen)

Mirme, A., Tamm, E., Mordas, G., Vana, M., Uin, J., Mirme, S., Bernotas, T., Laakso, L., Hirsikko, A. & Kulmala, M. 2007: A wide-range multi-channel Air Ion Spectrometer. *Boreal Env. Res.* 12: 247–264.

A new multi-channel air ion spectrometer (AIS) is presented. The instrument allows simultaneous measurements of positive and negative ion distributions from 3.2 to 0.0013 cm<sup>2</sup> V<sup>-1</sup> s<sup>-1</sup> (0.80–40 nm diameter or, using the Tammet correction, from 0.4 to 40 nm). The mobility range is divided into 27 fractions which are measured simultaneously to ensure a high time resolution (down to 10 seconds). The instrument calibration shows a good agreement with the mobility of electrically-classified, mono-dispersed aerosols. The spectrometer overestimates low concentrations of cluster ions. This is caused by a natural production of small ions (< 1 nm, 10 to 100 cm<sup>-3</sup>) inside the spectrometer. The instrument specifications, calibration results and measurements performed show a huge application potential of the new spectrometer.

### Introduction

Atmospheric aerosol particles affect natural ecosystems (Likens *et al.* 1996), human health (Davidson *et al.* 2005) and climate (Ramanathan *et al.* 2001, Lohmann and Feichter 2005). Their impact depends strongly on aerosol properties, such as the particle size distribution and chemical composition. The size distribution of the atmospheric aerosols is governed by nucleation, condensation, coagulation, deposition, in-cloud processes and by chemical reactions on particle surfaces. The first three of processes together constitute the so-called new-particle formation phenomenon, in which particles are produced from gaseous precursors by nucleation and grow subsequently by coagulation and condensation. The new-particle formation is one of the key

processes determining the existence of aerosol particles in the atmosphere. This phenomenon has been observed in various locations in the lower troposphere (e.g. O'Dowd *et al.* 1999, Birmili *et al.* 2003, Kulmala *et al.* 2004a). Many different theories have been proposed to explain the new-particle formation (Kulmala *et al.* 2000, Yu and Turco 2001, Laakso *et al.* 2002, Kulmala *et al.* 2006), and although this process has been studied for several decades, it is still not completely understood. This is because the newly-formed particles are very small and typically not detected by modern commercial instruments. Aerosol particle spectrometers have usually been able to observe particles with diameters larger than 3 nm. Some recent studies have shown the existence of smaller particles (e.g. Kulmala *et al.* 2005).

There exists a technique for measuring air ions which are either regular aerosol particles having an electric charge or molecular clusters stabilized by the Coulomb force of an electric charge. Air ion measurements provide information about the aerosol particles down to molecular clusters sizes.

A universal and widespread method for the measurement of air ion mobility distributions is the aspiration method. The method was first developed in the end of the 19th century (e.g. Thomson and Rutherford 1896). The general theory of the method and its practical realizations are described in the monograph by Tammet (1970). The aspiration method is often used in aerosol spectrometers which measure the mobility distribution of artificially charged particles. The particle size distribution (size spectrum) is calculated from the measured mobility distribution.

A regular aspiration spectrometer has one measurement channel. The mobility distribution is measured using scanning by a regime parameter (e.g., voltage on the aspiration spectrometer). The first commercial instrument based on the aspiration method was the EAA 3030 (Electrical Aerosol Analyzer), which was developed in 1966 (Whitby and Clark 1966). The EAA was replaced by the differential mobility particle sizer (DMPS) in 1983 (Keady *et al.* 1983). This instrument measures particle size distributions in the diameter range of 3 to 1000 nm. These instruments are of the scanning type with a typical measurement time of 10 to 20 minutes. The measurement time was reduced to two minutes with the scanning mobility particle spectrometer (SMPS), in which the classifying voltage continuously ramps up (Wang and Flagan 1990). The SMPS is still widely used to measure particle size distribution from 3 to 300 nm. The scanning limits the time resolution of the spectrometer and causes dynamic measurement uncertainties for fluctuating or rapidly changing particle concentrations.

A multi-channel measurement method eliminates the above-mentioned shortcoming. This method and corresponding ion mobility spectrometers (Tammet *et al.* 1973, Tammet *et al.* 1987) as well as the electrical aerosol spectrometer (EAS, Tammet *et al.* 2002) were designed

and developed at the University of Tartu. A multi-channel spectrometer measures all fractions of the particle spectrum simultaneously, thus obtaining the mean spectrum of the whole measurement time period. The size range measured by the EAS is 3.2 nm–10  $\mu\text{m}$ , which is similar to other commercial spectrometers.

The main limitation of the existing spectrometers is the lowest detectable size of about 3 nm. During the last four years a new version of the multi-channel air ion spectrometer (AIS) was developed and built by AIREL Ltd., a spin-off company of the University of Tartu. The unique design of the instrument allows the measurement of ion distributions of both polarities in a wide mobility range from 3.2 to 0.0013  $\text{cm}^2 \text{V}^{-1} \text{s}^{-1}$  or in the corresponding ion diameter range from 0.80 to 40 nm (based on Millikan). The mobility range is divided into 27 simultaneously measured fractions. In addition, the AIS needs no consumables and can, depending on the measuring environment, continuously monitor the air ion mobility distribution for months without the need for service. The new instrument can meet the requirements of many researchers and it may find different applications. The AIS has been used in aerosol particle nucleation research since 2003. The scientists of the University of Helsinki use it to measure ion mobility distributions during new-particle formation events. Measurements have been performed at many different locations around the world (Kulmala and Tammet 2007).

In this paper, we present the main specifications, design, operation principles and limitations of the AIS. We show a method for calibrating the spectrometer and present our calibration results. An additional investigation of the background was performed by using clean, particle- and ion-free air. The article presents different applications and measurements results of the new spectrometer.

## Instrument design

### Operation principles and construction

The spectrometer consists of two independent columns. In each column, the ions are classified

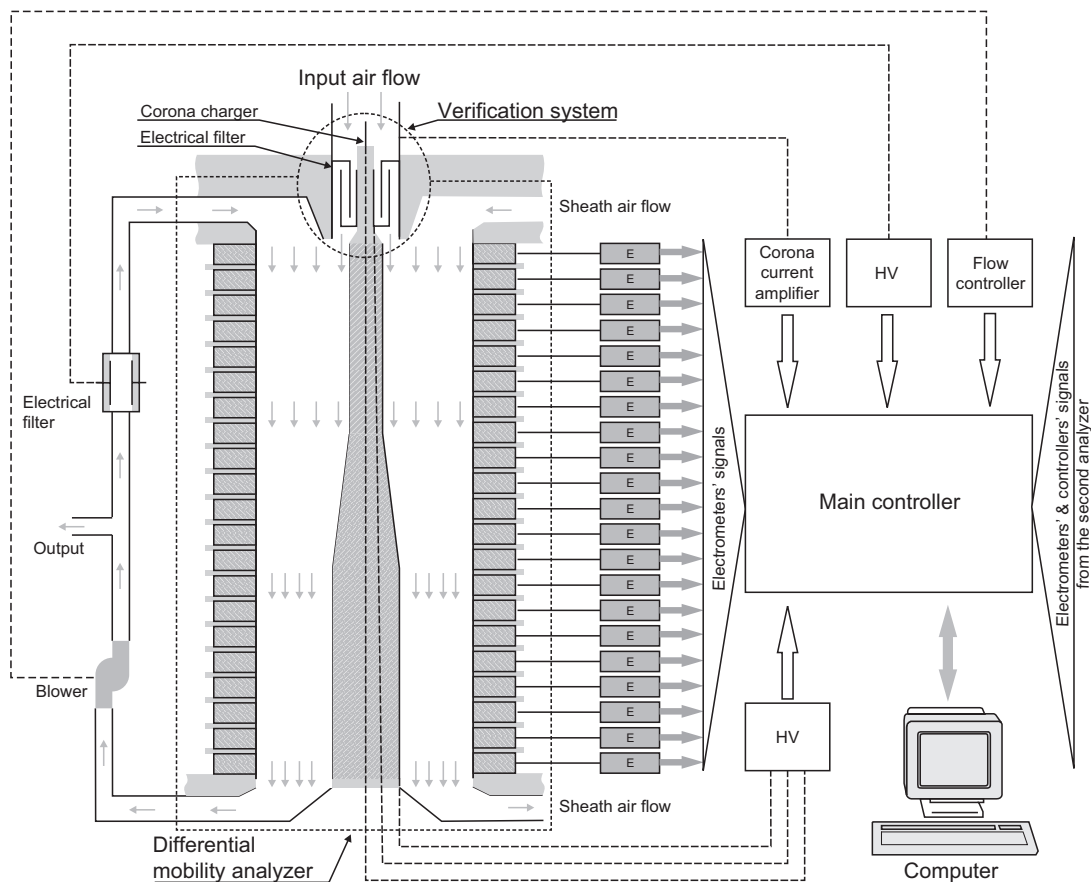


**Fig. 1.** The schematic design of air ion spectrometer AIS. Both columns of the spectrometer are symmetrical. The figure presents the detailed structure of one of them.

by a cylindrical differential mobility analyzer (DMA). The central electrode of the first analyzer is biased to positive electrical potential to measure positive ions and the electrode of the second analyzer is biased to negative potential to measure negative ions. Outer electrodes consist of a number of insulated sections, each having its own electrometer. The ions are simultaneously classified and collected to the sections, and ion currents are recorded by the electrometers. The multi-channel collecting system allows the measurement of quick changes in the ion concentration.

The general working principle and design of the AIS are shown schematically in Fig. 1. The ion-containing air is sucked into the spectrometer by a built-in, fan-type air pump (blower). The total input flow rate is  $1000 \text{ cm}^3 \text{ s}^{-1}$ . The entering air goes through an inlet tube and is divided into

two equal flows,  $500 \text{ cm}^3 \text{ s}^{-1}$  per each DMA. Both the flows pass the instrument verification system (this is used to confirm the bias current and noise level of the channels) and enter the DMA close to the inner electrode.

Clean sheath air with a flow rate of  $1000 \text{ cm}^3 \text{ s}^{-1}$  is injected through the set of laminarizing grids into the annular slit near the outer electrode. The clean air is obtained by recycling the DMA exhaust air, filtered by the DMA and complementary electric filters. Therefore, the gaseous phase parameters of the sampled ion-containing air and the sheath air are approximately the same. All airflows of the spectrometer are driven by a single blower.

The mobility analyzer is a cylindrical capacitor consisting of an ion-repulsive inner electrode and ion-collecting outer electrode. An inlet for the sample airflow and injector for the sheath

flow are located in its upper part. The collecting electrodes of the mobility analyzers are divided into electrically-isolated sections. All of these sections have an electrometric amplifier (electrometer). Each section, together with its electrometer, corresponds to one measuring channel of the spectrometer. One analyzer has 21 measuring channels, so the total number of the AIS channels is 42. The inner electrode is divided into sections. The three lowest sections have a cylindrical shape, whereas the other sections consist of two cylindrical parts of different diameters connected to each other with a conical part. All the parts are electrically isolated from each other. The sophisticated geometry and voltages of the sections enable the instrument to divide a very wide measurable mobility range into logarithmically nearly uniformly-distributed fractions. The design is based on the theory of the aspiration method (Tammet 1970).

The DMA generates a radial electrical field. The ions moving in the field precipitate onto different sections of the outer collecting electrode according to their mobility. The electric currents carried into these sections by ion fluxes are measured by electrometers.

### Measurement verification

The instrument is supplied with a verification system. The system is installed after the inlet tube and it consists of a corona charger and electrical filter. The verification system eliminates the impact of parasitic currents generated by the insulators of the sections of the collecting electrode and the zero drift of the electrometers. The input signals are periodically interrupted by switching on the charging and electric filtration of particles in the input air. The charger polarity is opposite to that of the analyser. This way, all particles getting into the differential mobility analyzer are either uncharged or have a polarity that is opposite to the analyser polarity, so that they do not cause a signal on the collecting electrodes. Opposite charging together with filtration eliminate the ion collection onto electrometer electrodes and makes it possible to measure electrometer currents in the absence of ion currents. This information is used to subtract

the parasitic currents from the measured electrometer currents and to maintain only the electric currents that are created by the ions of the sampled air. The corrected electrometer signals form the instrument record. The measurement uncertainties are also assessed from this procedure and they form the instrument error vector. The principal operation parameters, such as the rate of airflow, analyzer voltages and charging currents are regularly verified. The whole measurement process is controlled by a computer through the main controller.

### Measurement act

The duration of one measurement is controlled by software and it can be set from approximately ten seconds to several tens of minutes. The sensitivity and signal-to-noise ratio can be improved by lengthening the measuring time. A five-minute cycle for measuring natural atmospheric air ions is arranged by default. The structure of the default measurement cycle comprises 30 elementary spectrum acquisitions: 20 consecutive ten-second spectrum measurements followed by 10 measurements of the parasitic currents of the electrometer. However, the user can change the number of elementary measurements. In the end of the cycle, the mean spectra (including uncertainties) of ions of both polarities for this cycle are calculated from the mean channel signals and stored in a data file. The values of diagnostic parameters (analyzer voltages, flow rate, etc.) are also stored to allow for further analysis and checking of the quality of the measurements.

### Data inversion methods

The computer converts the measured electrometer signals into an ion mobility distribution using a special theoretical algorithm. The measurements of positive or negative ions can be described by a linear matrix equation. The transfer equation, also called as the instrument equation, apparatus equation or instrument response equation, is given by

$$\mathbf{y} = \mathbf{H}\phi + \Delta\mathbf{y}, \quad (1)$$

where  $\mathbf{y}$  is the instrument record (a vector of 21 electrometer signals),  $\Delta\mathbf{y}$  is the vector of the electrometer signal errors (21 elements),  $\mathbf{H}$  is the instrument matrix ( $21 \times 28$  elements) and  $\boldsymbol{\phi}$  is the spectrum vector (28 elements). The spectrum vector is a set of spectrum values at certain mobility bins, which are distributed uniformly on the logarithmic scale of the spectrum argument, i.e. the electrical mobility of air ions. The number of mobility bins is 28. It is a matter of compromise between the ability of a distribution to follow the cluster ion peak and its susceptibility to random measurement errors. Each element of the spectrum vector,  $\phi_i$ , represents a superposition of the 28 predefined elementary spectra  $f_i$  with the coefficients  $\beta_i$ . The predefined 28 elementary spectra form the fractions on the electrical mobility scale, which are presented in the Table 1. The instrument channels, conformable to the mobility fractions and their corresponding Millikan diameters, are shown in Table 2.

**Table 1.** The electrical mobility fractions of AIS.

Fraction number	Mobility range (cm <sup>2</sup> V <sup>-1</sup> s <sup>-1</sup> )	Mean mobility (cm <sup>2</sup> V <sup>-1</sup> s <sup>-1</sup> )
1	3.1623–2.3714	2.76685
2	2.3714–1.7783	2.07485
3	1.7783–1.3335	1.55590
4	1.3335–1.0000	1.16675
5	1.0000–0.7499	0.87495
6	0.7499–0.5623	0.65610
7	0.5623–0.4217	0.49200
8	0.4217–0.3162	0.36895
9	0.3162–0.2371	0.27665
10	0.2371–0.1778	0.20745
11	0.1778–0.1334	0.15560
12	0.1334–0.1000	0.11670
13	0.1000–0.0750	0.08750
14	0.0750–0.0562	0.06560
15	0.0562–0.0422	0.04920
16	0.0422–0.0316	0.03690
17	0.0316–0.0237	0.02765
18	0.0237–0.0178	0.02075
19	0.0178–0.0133	0.01555
20	0.0133–0.0100	0.01165
21	0.0100–0.0075	0.00875
22	0.0075–0.0056	0.00655
23	0.0056–0.0042	0.00490
24	0.0042–0.0032	0.00370
25	0.0032–0.0024	0.00280
26	0.0024–0.0018	0.00210
27	0.0018–0.0013	0.00155

The shape and number of the elementary spectra are chosen according to the approximation and calculation accuracy of the instrument for a typical atmospheric aerosol/ion distribution. The elementary spectra have a mode at the corresponding mobility bin and the value of 1 at the bin. By such a choice of the elementary spectra  $\beta_i = \phi_i$ . In essence, the spectrum vector  $\boldsymbol{\phi}$  is a continuous ion mobility distribution density function. The respective conversion is performed using a converter matrix. The converter matrix ( $\mathbf{H}$  in Eq. 1) is calculated so that the result of the solution of Eq. 1 is the density function of the ion mobility distribution. The converter also defines the mobility bins at which the distribution density has been calculated. The distance between the mobility bins is considered small enough, so that the intermediate distribution density values can be approximated with a straight line.

The instrument equation can be solved by the Gauss-Markoff least squares method:

$$\boldsymbol{\phi} = (\mathbf{H}^T \mathbf{D}^{-1} \mathbf{H})^{-1} \mathbf{H}^T \mathbf{D}^{-1} \mathbf{y}. \quad (2)$$

**Table 2.** The distribution of the mean mobilities and corresponding Millikan diameters by the instrument channels.

Channel number	Mean particle diameter (nm)	Mean mobility (cm <sup>2</sup> V <sup>-1</sup> s <sup>-1</sup> )
1	0.900	2.4200
2	1.040	1.8200
3	1.200	1.3600
4	1.380	1.0200
5	1.600	0.7660
6	1.860	0.5750
7	2.140	0.4310
8	2.480	0.3240
9	2.860	0.2420
10	3.300	0.1820
11	3.820	0.1360
12	4.420	0.1020
13	5.100	0.0766
14	6.820	0.0431
15	9.140	0.0243
16	12.240	0.0136
17	16.460	0.0077
18	22.160	0.0043
19	29.900	0.0024
20	38.000	0.0019
21	42.000	0.0010

Here  $\mathbf{D}$  is the covariance matrix of the instrument record ( $21 \times 21$  elements). As a rule,  $\mathbf{D}$  is a diagonal matrix, the elements of which are the variances of the output signals, and  $(\mathbf{H}^T \mathbf{D}^{-1} \mathbf{H})^{-1}$  is the co-variation matrix of the spectrum and its diagonal elements give the random uncertainties (variances) of the components of the spectrum vector. The inversion is performed using the Tikhonov regularization (Tikhonov 1963). The method makes it possible to reduce the rank of the matrix and thus to correct the ill-posedness (Lemmetty *et al.* 2005).

The uncertainties in the ion mobility distribution density function are calculated from the spectrum covariance matrix using the converter. The 27 fraction number concentrations (integral of the density function between adjacent mobility bins) and their uncertainties can be calculated from the number distribution density. These calculations are carried out in real-time for the AIS. The number of the fractions has been chosen according to the real resolution of the instrument: eight fractions per a decade of the particle mobility.

The instrument matrix  $\mathbf{H}$  has been determined by a calibration procedure based on the mathematical model of the spectrometer and experiments for assessing the input losses. This process is similar for both columns. There are two instrument records of 21 elements each, and two instrument matrixes of  $21 \times 28$  elements processed in parallel.

## Calibration methods and materials

The principal information of a multi-channel spectrometer (AIS) is presented with an instrument equation (Eq. 1). The equation determines the  $28 \times 21$  elements of the instrument matrix  $\mathbf{H}$ . The matrix  $\mathbf{H}$  describes the transformation of the information in the spectrometer — it is a generalized linear response of a multi-channel instrument. The mathematical model of the AIS is less complicated than that of the EAS because ions are measured without intermediate steps as is done with the EAS in order to achieve charge equilibrium (Mirme 1987, Tammet *et al.* 2002). In the EAS, the particles are charged,

their mobility distribution is measured, and then their size distribution is calculated by an inversion procedure. The response of the AIS and thereby its instrument matrix can be calculated quite well based on measured geometric, electric and regime parameters. Each section of the mobility analyzer can be treated as a differential aspiration condenser of the second order and the respective theory can be applied (Tammet 1970). The responses of the channels overlap. This is considered and corrected by the data inversion.

The measurement range of the AIS covers air ions of different physical nature: cluster ions and aerosol ions. The mobility range of the cluster ions is  $3.2\text{--}0.5 \text{ cm}^2 \text{ V}^{-1} \text{ s}^{-1}$ , which corresponds to the particle mass diameter (with the Tammet correction) range of  $0.4\text{--}1.6 \text{ nm}$  at  $20 \text{ }^\circ\text{C}$ . The respective ranges for aerosol ions are  $0.4\text{--}0.0013 \text{ cm}^2 \text{ V}^{-1} \text{ s}^{-1}$  and  $1.6\text{--}40 \text{ nm}$  (with the Tammet correction) (Hörrak *et al.* 2000).

All the analyzer parameters are measured with an accuracy better than 1%. The most poorly-determined parameter is the ion loss at the spectrometer inlet, which may have a significant effect on fast ions. On the other hand, the parameters of the calibration aerosols are defined with the accuracy of about 10%, except for cluster ions. Well-defined calibration ions are not available in this range. Therefore, the analyzer calibration consists mainly of verification with the classified aerosol and the experimental calibration for the assessment of diffusion losses in the input tract.

## Instrument calibration in the aerosol ion range

Known calibration methods of multi-channel aerosol size spectrometers (Mirme 1987, Tammet and Noppel 1992) can be used for the aerosol ion range. We applied the mobility-classified monodispersed aerosols of a well-defined mobility distribution (approximately lognormal size distribution with known mean diameter, number concentration and standard deviation). The AIS is not an instrument having a high mobility resolution (fraction width  $\sim 30\%$ ). As a result some deviation of the classified aerosol from a real log-normal one has little effect.

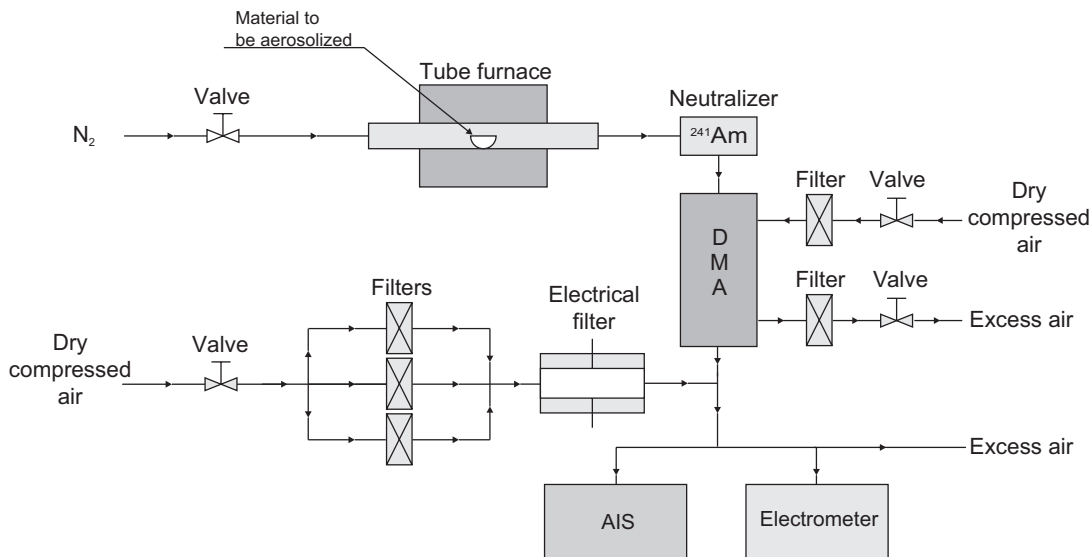


Fig. 2. The calibration setup of the air ion spectrometer at the University of Helsinki.

A rough initial calibration was performed by simulating the response of the spectrometer using the measured or some arbitrary values for the parameters. The calibration was refined by comparing the simulation with the data of the calibration experiments. These were performed at two locations: the University of Helsinki and the University of Tartu. The calibration aerosols were prepared using the classical method of electrical classification (Liu and Pui 1974). Nanometre-size silver particles for the classification were prepared by the evaporation-condensation method (Scheibel and Porstendörfer 1983).

#### Calibration setup at the University of Helsinki

The experimental setup at the University of Helsinki is shown in Fig. 2. A polydispersed aerosol sample was produced by a tube furnace (Carbolite Furnaces MTF 12/388). The furnace heated a ceramic tube. A ceramic cup with silver powder was installed inside the tube. The silver was evaporated into the passing nitrogen flow. As the flow cooled down outside of the heated section of the furnace, the vapour nucleated and formed polydispersed aerosol particles. The size distribution of the aerosol is a function of the

residence time within the heated section and temperature. The residence time was constant during the experiments, whereas the particle size distribution was optimized for each measurement by varying the temperature between 1050 and 1200 °C. The nitrogen flow rate through the furnace tube was 3.0 l min<sup>-1</sup>.

The aerosol was charged with an alpha-active <sup>241</sup>Am (60 MBq — 1995/03) bipolar source, after which a mono-dispersed fraction of the aerosol was selected using a DMA (VIE-08, Hauke, length 0.109 m). The DMA was operated with a flow rate of 3.0 l min<sup>-1</sup> for the aerosols and the flow rate of 20.0 l min<sup>-1</sup> for the sheath and excess airflows in an open-loop arrangement. The flows were measured with a Gillian bubble flow meter and controlled with needle valves. The classification voltages were set manually with accuracy of 0.1 V.

The classified mono-dispersed aerosol was diluted with clean (particle and ions free) air. The dilution air was produced by cleaning dry compressed air. The cleaning was performed with three parallel HEPA filters and finalised by an electrical filter. The flow rate of the dilution air was 70 l min<sup>-1</sup> and the flow rate of the mobility-classified aerosol was 3.0 l min<sup>-1</sup>. The diluted aerosol sample was directed into the AIS and aerosol electrometer (TSI 3068). The flow rates

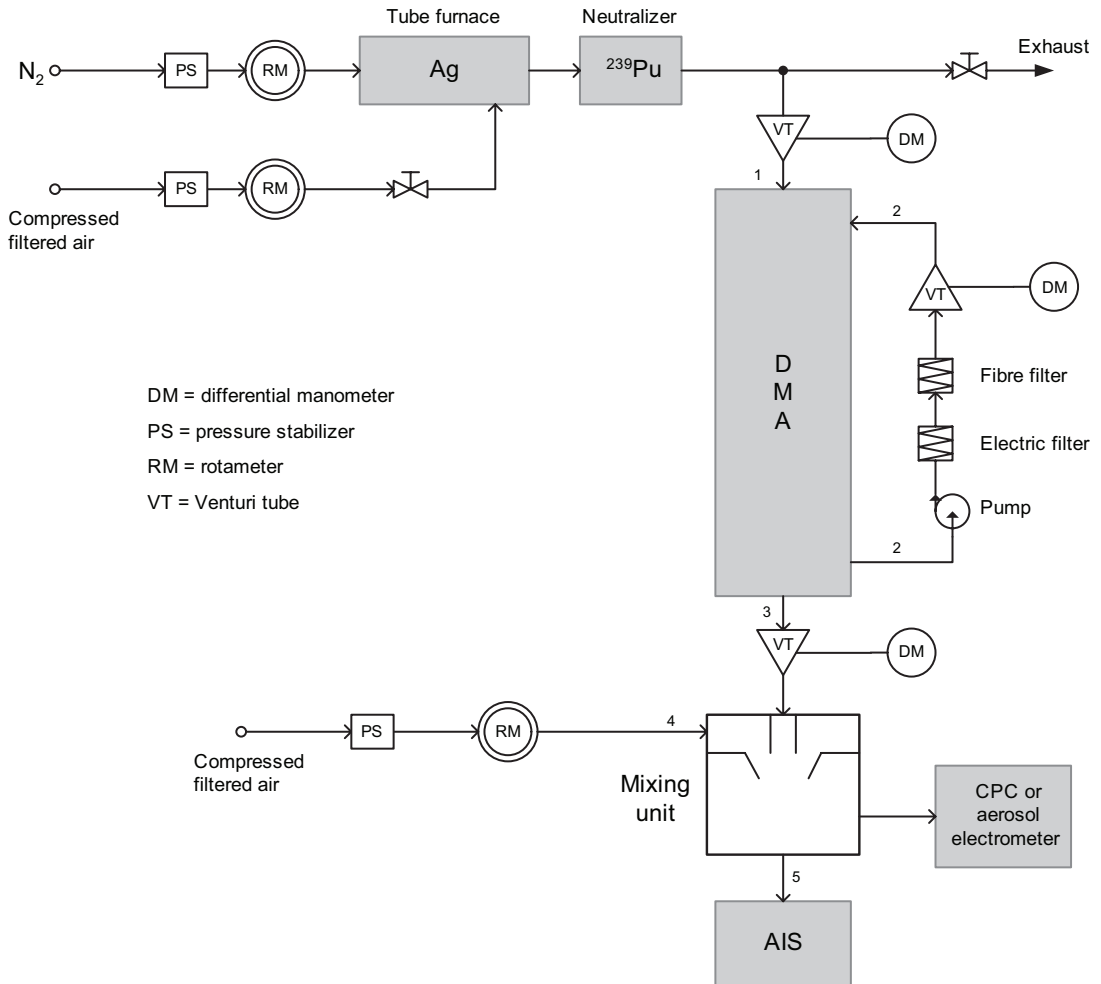


Fig. 3. The calibration setup of the Tartu University.

of the AIS and electrometer were  $60$  and  $3.75$   $\text{l min}^{-1}$ , respectively. All excess air was directed away, which guaranteed a normal atmospheric pressure (no pressure loading) on the inlet of the spectrometer.

#### Calibration setup at the University of Tartu

The calibration setup of the University of Tartu (Fig. 3) is mostly similar to that of the University of Helsinki, with some minor differences. For the smallest particles (diameter  $< 15$  nm), a tube with a nozzle was used in the furnace. Silver vapour containing nitrogen that exited the nozzle

was immediately mixed with cool air in order to stop the condensational growth of nucleated particles. The nitrogen flow rate was varied from  $1$  to  $3.3$   $\text{l min}^{-1}$ , the diluting air flow rate ( $\Phi_4$ ) was  $13$   $\text{l min}^{-1}$ . In the charger, a  $^{239}\text{Pu}$  neutralizer was used. The input and output aerosol flow rates ( $\Phi_1$  and  $\Phi_3$ , respectively) of the self-designed Vienna-type DMA were  $2.5$   $\text{l min}^{-1}$ . The sheath air with a flow rate of  $25$   $\text{l min}^{-1}$  was prepared by filtering the excess air (closed-loop arrangement). The aerosol from the DMA was mixed with the filtered air in a mixing unit with a semi-open exit, so that  $\Phi_3 + \Phi_4 > \Phi_5$  and the DMA output and the AIS input flows ( $\Phi_5$ ) were self-maintained. All the flow rates were continuously

controlled by rotameters or by Venturi tubes and differential manometers.

### Instrument calibration in cluster ion range

A calibration procedure similar to that presented above could have been used in the cluster ion range if mono-mobile cluster ions were available. The mobility distributions of the natural cluster ions change very fast, so that the separated mono-mobile fraction of ions will quickly develop into a stationary mobility distribution for given meteorological and air chemical composition conditions. Up to now, we have not adopted the method of electrospraying of solutions of polymers and other organic substances, and the subsequent classification of the  $n$ -mers (the molecules of the  $n$ -polymers) by the DMA with a very high resolution (e.g. Rosell-Llompart *et al.* 1996). In the cluster ion range, the AIS was calibrated by comparing the total concentrations of cluster ions measured by the AIS and by the improved version of the integral ion counter SAI-TGU (Tammet 1970). The SAI-TGU has a very simple and short input tract and high input flow rate ( $4.5 \text{ l min}^{-1}$ ). It was thoroughly investigated by Tammet (1970), so it can be considered as an absolute ion concentration measurement device. Furthermore, we have compared the AIS with the BSMA, another ion spectrometer designed at the University of Tartu (Tammet 2006).

### Calibration results and discussions

The AIS has several important characteristics, including a high spectrometer resolution, low instrumental background for concentrations, and a stable and long operation time. The resolution is defined by the ion classification process inside the differential mobility analyzer and the mathematical conversion that results in a mobility distribution. A two-stage investigation was performed for this. In the first stage, we studied the signal distribution along the instrument channels using mobility-classified, mono-disperse, charged aerosol particles (calibration aerosols).

In the second stage, we converted the measured signal distribution to a mobility distribution and compared the result with the expected distribution of the calibration aerosol. The calibration aerosol was produced with the calibration setups, as described in the previous section (Figs. 2 and 3). The broadening of the distribution by diffusion was considered small.

### Investigations of the signal distribution

We investigated the signal distribution using negatively charged calibration aerosol particles. The selected particles had median diameters of 3, 4, 5, 6, 8, 10 and 20 nm. A typical signal distribution by instrument channels is presented in Fig. 4. It can be seen that the signals of the channels spanned four orders of magnitude from  $-0.02$  to  $-50 \text{ fA}$ . A background signal of about  $-0.4 \text{ fA}$  in the channels analyzing the cluster ions is indicated with the gray shaded area. It seems that the signal values lower than  $0.4 \text{ fA}$  could have been affected by the instrument background signals. Nevertheless, the background level of the signal was less than 1% of the maximum level. The dynamic range was even wider with the cluster ion background correction. Compared with cluster ion channels, the background was lower at aerosol particle channels. So, using mono-disperse, single-charged particles, the signal was above the background level in only a few channels. For example, the signal of 4 nm negatively-charged particles was distributed over five channels (channels 30–34; Fig. 4). The relative signal distribution over channels was symmetrical with a peak on the channel 32 (bars in Fig. 4). This peak was strong and consisted of 50% of the total measured signal. The two nearest channels (31 and 33) had 23 and 25% of the total measured signal, respectively, and the other channels had less than 10% of the total measured signal. Thus, up to 90% of all particles of the calibration aerosol were accumulated on three channels.

When using different-size calibration aerosols, we analyzed only the channels that had more than 10% of the total measured signal (Table 3). It can be concluded that the particles accumulated on several channels. The signal

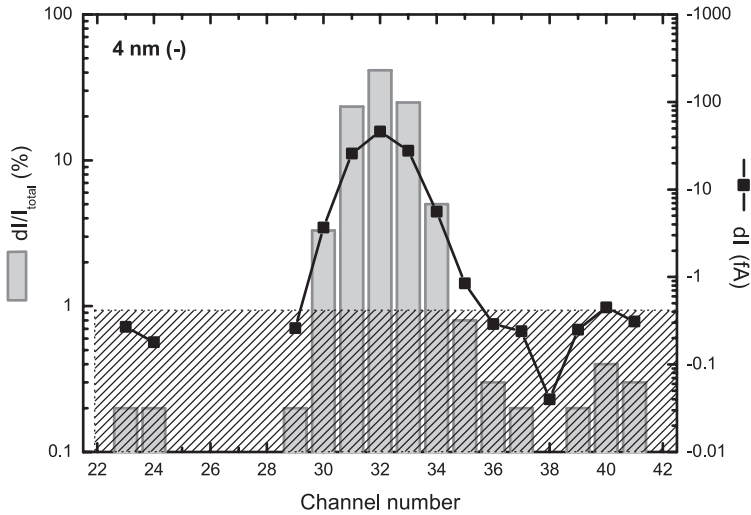


**Fig. 4.** The current distribution over the instrument channels. The data in bars gives the relative current distribution (left-hand-side scale). The right scale characterizes the absolute current distribution presented with a line with squares. The shaded area indicates the background.

distribution was wider at smaller particle sizes, while larger particles accumulated only onto two channels.

### Investigations of the mobility distribution

The measured signal distribution was converted into a mobility distribution using a mathematical algorithm based on Eq. 2. The mathematical algorithm is included in the instrument software which controls the operation of the instrument and saves the measured and converted data. This enables one to reanalyse the measurement data later. The measured signal distribution of the calibration aerosol used in the first experi-

**Table 3.** The modes of the channel current distribution using calibration aerosol. The first column presents the modal size of the used calibration aerosol and second column gives the channel numbers with more than 10% of the total measured current. The channel having the peak of the current distribution is marked with boldface.

Particle diameter (nm)	Channel number
20	<b>25–26</b>
10	<b>28–29</b>
8	<b>29–30</b>
6	<b>30</b>
5	<b>30–31–32</b>
4	<b>31–32–33</b>
3	<b>33–34–35</b>
2	<b>34–35–36–37–38</b>

ment was converted into a mobility distribution. After that, the converted mobility distribution was compared with the mobility distribution of the classified calibration aerosol. The mobility distribution of the calibration aerosol was described by the transfer function of the classified DMA. The transfer function was calculated based on the operation characteristics of the DMA including the diffusion effects of small particles (Stoltzenburg 1988). We made a comparison between the mobility distribution of the calibration aerosol and the corresponding converted mobility distribution of the AIS normalized to the total measured ion concentration (Fig. 5). Both distributions seemed to have the same mobility peak. However, the converted mobility distribution was wider and the height of the peak was lower. Additionally, the converted distribution was asymmetrical, indicating that it contained about 5% of particles of smaller sizes. The existence of small particles is unlikely and can be explained by the background of the instrument.

The AIS has been regularly verified with the calibration setup at the Universities of Helsinki and Tartu using classified mono-dispersed aerosols. Figure 6 presents the estimated Millikan particle size versus the classified size of about 200 spectra of both polarities. The background cluster concentration below 1.5 nm sizes was set to zero. The particle size was underestimated on average by 4% and the scatter (STD) was

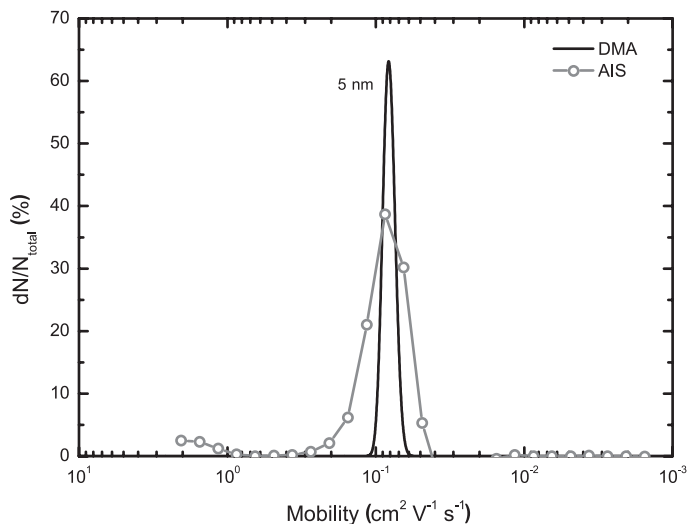


**Fig. 5.** The mobility distribution using calibration aerosol. The line presents the transfer function of the DMA used to select mono-disperse aerosol. The curve with circle-points shows the mobility distribution measured by the AIS.

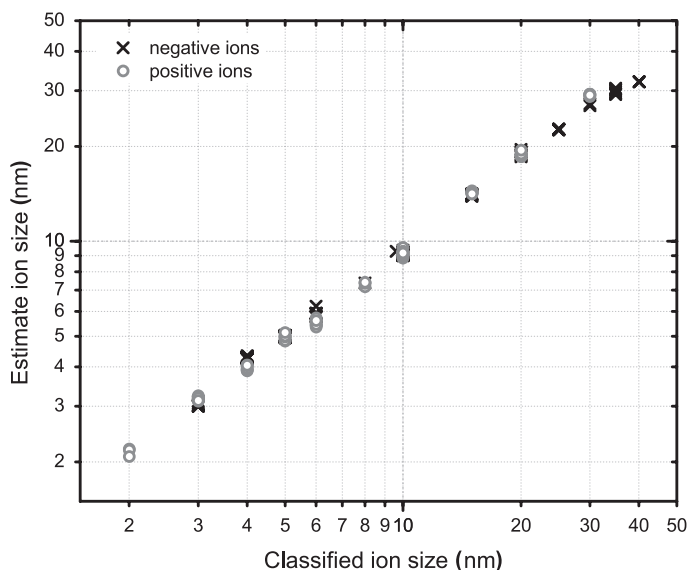


**Fig. 6.** The comparison of the AIS particle sizing. The size was estimated based on Millikan or measured with the AIS.

6% of the size. The sizes above 35 nm deviated because a part of the distribution was beyond the measurement range. The calibration aerosol number concentrations ranged from 80 to 20 000 particles  $\text{cm}^{-3}$ . The ratio of the estimated concentration to the expected one is presented in Fig. 7. The concentrations were underestimated on average by 12% and the scatter (STD) was 20%. The obvious reason for this is that the estimated uncertainties in the concentrations of calibration aerosols were larger than those in their size, and that there were possible uncertainties associated with the inversion procedure.

## Instrument background

The background study was performed using a modified calibration setup presented in Fig. 2. In the modified setup, the DMA was disconnected from the AIS and the AIS used only dry compressed air from the cleaning system. The compressed air was cleaned with three parallel-connected HEPA filters and existing air ions were eliminated with an electrical filter. Thus, all particles and ions were filtrated and the AIS measured its background. The duration of the experiment was 24 hours. The daily mobil-

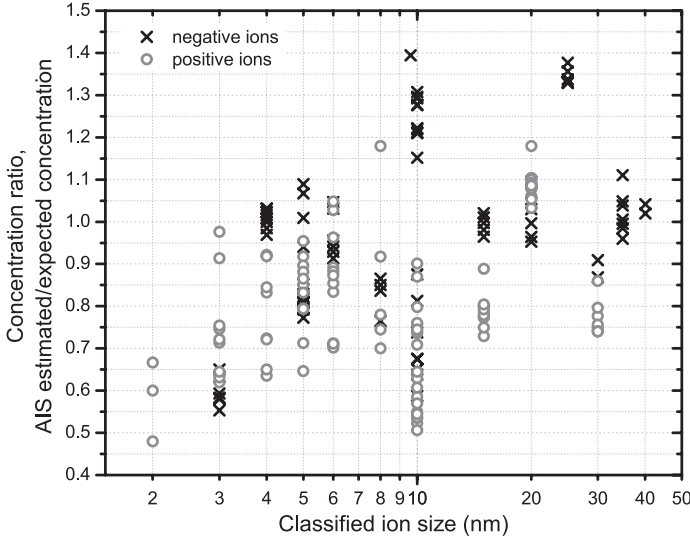


**Fig. 7.** The relative deviation of measured aerosol concentrations by AIS.

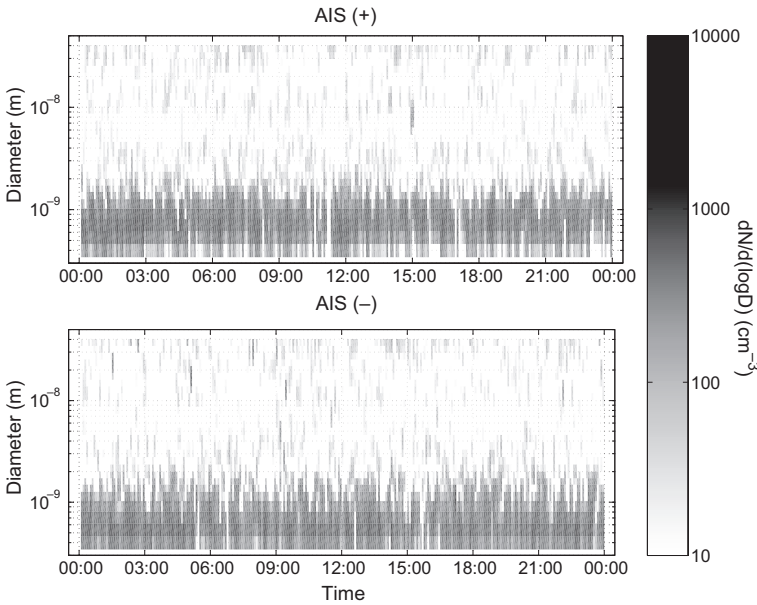


**Fig. 8.** The daily distributions of the measured ion background of the AIS for positive (top) and negative (bottom) ions.

ity distributions of negative and positive ions during the background experiment are shown in Fig. 8. Small positive and negative ions were observed during the experiments. Their number concentration was fluctuating. The daily averaged number concentrations are presented in Fig. 9, showing that the number concentration of the particles larger than one nanometre was less than  $4 \text{ cm}^{-3}$ . However, smaller ions were present in the instrument all the time and their number concentration was in the range  $10\text{--}100 \text{ cm}^{-3}$ . The

existence of the background can be explained by the production of cluster ions inside the AIS. The natural ion production, with the rate of about  $10 \text{ pairs cm}^{-3} \text{ s}^{-1}$  or less in the atmosphere, may be higher inside the instrument due to the presence of radioactive materials, mainly radon and its daughters, inside the inlet tube. The ion production goes on always and everywhere and cannot be completely avoided. The background can be corrected by subtracting the mean background in the cluster ion mobility range.

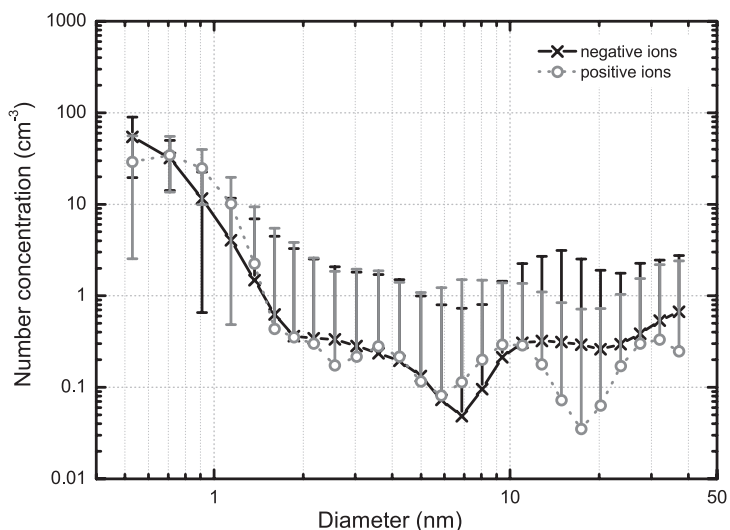


**Fig. 9.** The daily averaged ion background of the spectrometer for negative and for positive ions.

### Instrument comparison with an ion counter using cluster ions

A special setup was built for altering ion concentrations in the input air in order to check the calibration of the AIS in the cluster ion sub-range. The air blown through the  $^{239}\text{Pu}$  charger-neutralizer (Fig. 3) was mixed with normal room air and conducted to the input orifices of the AIS and the ion counter SAI-TGU, located side by side. The limiting mobility of the ion counter was chosen so that only cluster ions were measured.

The AIS measured higher concentrations than the SAI-TGU at low ion concentrations (Table 4), which is caused by the background generated inside the AIS. This enables the assessment of the background ion concentration and correction of the measurement results (two last columns in Table 4). Curves in Fig. 10 characterize the ion losses in the input arrangements of

the AIS depending on ion concentrations. The losses are higher at higher concentrations due to the dependence of the recombination rate ions on their concentration. The losses have been taken into account by later post-processing of the data.

### Instrument working parameters

The working parameters were analysed during a long-term running of the AIS. The parameters that characterise the working of all the main components of the spectrometer are the total entering flow rate, the high voltages of the differential mobility analyzers and electrical filter currents. Aspiring to get better resolution of the spectrometer, the differential mobility analyzer generates an electrical field of complicated geometry (*see* the section “Instrument design”) with four different high voltages. The nominal values of the

**Table 4.** Concentrations of cluster ions ( $\text{cm}^{-3}$ ) in the mobility range  $3.2\text{--}0.5 \text{ cm}^2 \text{ V}^{-1} \text{ s}^{-1}$  measured by the AIS and SAI-TGU. +/– in the parentheses refer to positive/negative ions.

Experiment	SAI-TGU (+)	AIS (+)	SAI-TGU (–)	AIS (–)	AIS (+), corrected	AIS (–) corrected
1	6900	5300	5180	4380	5060	3940
2	4940	3830	3800	3450	3590	3010
3	2960	2550	2310	2340	2310	1900
4	1420	1567	1050	1420	1330	973
5	600	840	410	850	600	410

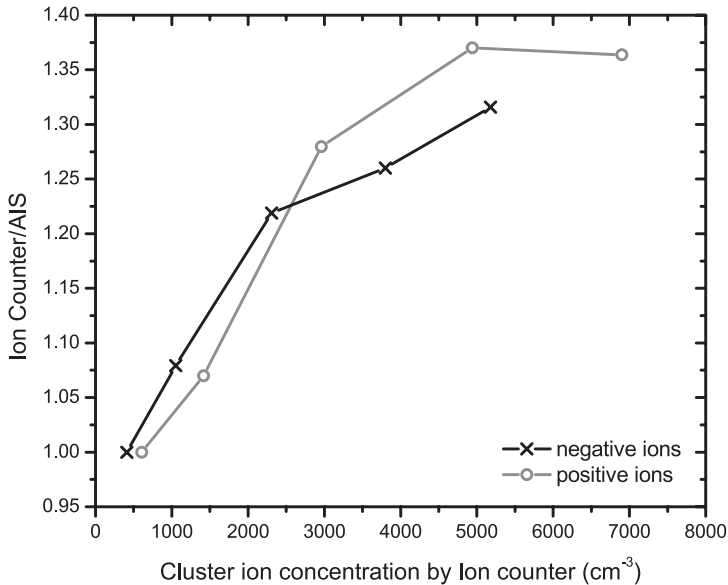


**Fig. 10.** The comparisons of AIS with the air ion counter SAI-TGU in the cluster ions sub-range (mobilities 0.5–3.2 cm<sup>2</sup> V<sup>-1</sup> s<sup>-1</sup>)

main working parameters are presented in Table 5. The fluctuations of these parameters during 24 hours were checked. The fluctuations of high-voltages did not exceed 0.1%. The current of the electrical filter is not as stable as fixed voltages, because its absolute value depends on the working conditions of the instrument and can have small variations during longer time. Experiments showed that fluctuations in the filter current were about 1%. However, they were different for positive and negative analyzers. This difference can be explained by a non-uniform deterioration of the used corona needles during the ion production. Fluctuations in the filter current do not affect stable working of the instrument. Periodical variations can be observed for the total flow rate. For a 42-hour period, the amplitude of fluctuations was about 2.5 cm<sup>3</sup> s<sup>-1</sup>, which is only 0.1% of the total flow rate of 991 cm<sup>3</sup> s<sup>-1</sup> (approximately 1% deviation from the nominal value).

## Applications and measurement results

The unique design of the AIS allows its use in specific experiments and different environments. The AIS has a wide measuring range according to 0.80–40 nm (Millikan diameters), or 0.42–40 nm (Tammets diameters). This size range contains clusters, nucleated aerosol particles and part of Aitken mode particles (Fig. 11). At present, the AIS is the only instrument that measures the ion size distribution in such a wide size range. An alternative instrument, the BSMA (Tammets 2006), can only measure in the range from 0.4 nm (Millikan size 0.8 nm) to 7.5 nm. Additionally, the constructed spectrometer has a wide concentration range from below 1 to several millions ions cm<sup>-3</sup>, while the time resolution of the spectrometer is from ten seconds to several tens of minutes. The combination of all these specifications gives the possibility to measure

**Table 5.** The nominal values of the main operation parameters of the air ion spectrometer AIS.

Flow rate (cm <sup>3</sup> s <sup>-1</sup> )	1000	
	Positive ion analyser	Negative ion analyser
Voltage (V) of four insulated sections of the analyzer	9, 25, 220, 800	-9, -25, -220, -800
Electrical filter voltage (V)	1200	-1200
Electrical filter current (fA)	-210	170

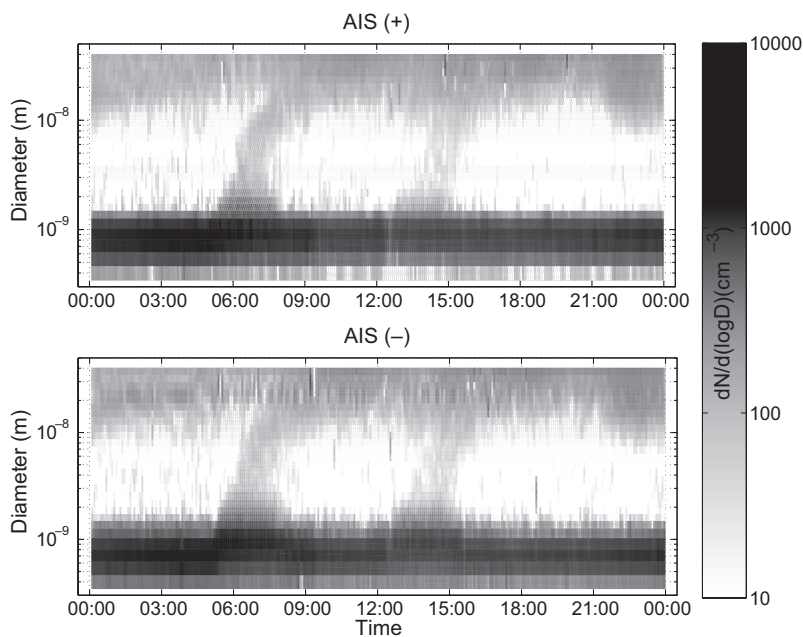


**Fig. 11.** The daily ion size distribution measured by the air ion spectrometer at the University of Helsinki at 16 November 2005. The ion size distribution is presented using Tammet diameters.

quick changes in ion size distributions of both polarities over a wide concentration range during long-term experiments.

Initially, the AIS was specially constructed for continuous monitoring of the atmospheric ion size distributions. The main application of the instrument is air monitoring at different locations (cities, rural and marine environments). Since 2003, continuous ion distribution measurements have been carried out at the SMEAR II station in southern Finland. Measurements of ion distributions have been conducted in Tartu, Estonia, episodically since 1985 and continuous ion mobility distribution measurements have been performed at the Tahkuse Air Monitoring Station of the University of Tartu since 1988 using a self-made system of ion mobility spectrometers (Hörrak *et al.* 2000). Short-term (several months) measurements have been carried out at many locations all over the world.

The largest database of the atmospheric ion size distributions has been collected at the University of Helsinki based on AIS measurements. Most of the measurements have been performed in a boreal forest at the SMEAR II research station. Using the database, researchers have made a statistical characterisation of concentrations of cluster ions and naturally-charged, nanometre-

size aerosol particles, in addition to which they have determined the ion sinks for the nucleation event days and non-event days (Hörrak *et al.* 2005). In addition, the charging state of the atmospheric nanometre-size particles has been investigated (Vana *et al.* 2006a). Laakso *et al.* (2004) estimated ion production rates based on ion mobility distributions and aerosol particle size distributions. Subsequent studies on the characterization of the initial steps of the aerosol particle growth have been conducted (Kulmala *et al.* 2004b).

The researchers from the University of Helsinki, in cooperation with the researchers of the University of Tartu, have performed ion distribution measurements in other environments as well. Experiments have been conducted on the coastal area of Antarctica (Virkkula *et al.* 2007) and over the Atlantic Ocean (Virkkula *et al.* 2005). The AIS was installed in the Alps mountain range in Switzerland (Vana *et al.* 2006b) and on the hills of Lapland (Ruuskanen *et al.* 2004). The performed experiments allowed the characterisation of different environments and they have offered a better understanding of the nucleation processes in the real atmosphere.

The most courageous experiments have been performed using a hot air balloon. The research-

ers installed the AIS in the cabin of the hot air balloon and performed measurements during flights over a boreal forest. Simultaneous ion distribution measurements were performed on the ground. As a result, vertical profiles of ion distributions during a nucleation event were obtained (Laakso *et al.* 2007).

## Summary and conclusions

This article presents a new air ion spectrometer (AIS). The unique design of the instrument allows simultaneous measurements of ion distributions of both polarities over a wide mobility range of  $3.2\text{--}0.0013\text{ cm}^2\text{ V}^{-1}\text{ s}^{-1}$ , which corresponds to a Millikan diameter range of 0.8–40 nm. The mobility distribution is presented by 27 logarithmically uniformly distributed fractions. All ions in the whole size range are measured simultaneously ensuring a high time resolution of the measurements and the ability to observe highly fluctuating ion concentrations. The concentration range of the spectrometer is from below 1 to several millions ions  $\text{cm}^{-3}$ . The combination of all these specifications presents huge possibilities for the applications of the newly-developed air ion spectrometer.

The article describes the design of the AIS, its main specifications, instrument calibrations and testing. The calibrations of the signal and the mobility distribution were performed using mobility-classified, mono-dispersed aerosols (calibration aerosol). The results showed a good agreement with the mobility of the selected calibration aerosol. In addition, the study of the ion background was performed using dry, compressed particle- and ion-free air. Experimental results showed the existence of ions smaller than one nanometre in diameter. Their concentration varied from 10 to 100  $\text{cm}^{-3}$ . The existence of the background can be explained by the production of small ions inside the instrument and by physical processes, which depend on the spectrometer's design and the stability of the main working parameters. The stability of the main parameters (flow rate, high voltages of analyzers, electrical filter voltages and current) were also investigated. No variations in excess 0.1% were found.

The instrument specifications and results of the performed studies confirm that the new air ion spectrometer, AIS, can find many different applications. It has already been used in many scientific experiments in nucleation research, and it monitors air ion mobility distributions at environmental stations at different locations all over the world.

*Acknowledgements:* We wish to thank our colleagues from the Air Electricity Laboratory of the Department of Environmental Physics of the University of Tartu and our colleagues from the Division of the Atmospheric Sciences of the Department of the Physical Sciences of the University of Helsinki for discussions of the problems and technical support. The construction, testing and research were supported in part by the Estonian Science Foundation under the grants no. 5387, no. 5855 and no.6988, and in part by the Academy of Finland and particularly by Nordic Centre of Excellence, BACCI.

## References

- Birmili W., Berresheim H., Plass-Dülmer C., Elste T., Gilge S., Wiedensohler A. & Uhrner U. 2003. The Hohenpeisenberg aerosol formation experiment (HAFEX): a long-term study including size-resolved aerosol,  $\text{H}_2\text{SO}_4$ , OH, and monoterpenes measurements. *Atmos. Chem. Phys.* 3: 361–376.
- Davidson C.I., Phalen R.F. & Solomon P.A. 2005. Airborne particulate matter and human health: a review. *Aerosol Sci. Technol.* 39: 737–749.
- Hörrak U. 2001. *Air ion mobility spectrum at a rural area*. Ph.D. thesis, University of Tartu, Tartu.
- Hörrak U., Salm J. & Tammet H. 2000. Statistical characterization of air ion mobility spectra at Tahkuse Observatory: classification of air ions. *J. Geophys. Res.* 105: 9291–9302.
- Hörrak U., Miller F., Mirme A., Salm J. & Tammet H. 1990. Air ion observatory in Tahkuse: instrumentation. *Acta et comm. Univ. Tartuensis* 880: 33–43.
- Hörrak U., Aalto P.P., Salm J., Mäkelä J.M., Laakso L. & Kulmala M. 2005. Characterization of air ions in boreal forest air during BIOFOR III campaign. *Atmos. Chem. Phys. Discuss.* 5: 2749–2790.
- Keady P.B., Quant F.R. & Sem G.J. 1983. Differential mobility particle sizer: a new instrument for high-resolution aerosol size distribution measurement below  $1\text{ }\mu\text{m}$ . *TSI Quarterly*. 9: 3–11.
- Kulmala M., Pirjola L. & Mäkelä J.M. 2000. Stable sulphate clusters as a source of new atmospheric particles. *Nature* 404: 66–69.
- Kulmala M., Vehkamäki H., Petäjä T., Dal Maso M., Lauri A., Kerminen V.-M., Birmili W. & McMurry P.H. 2004a. Formation and growth rates of ultrafine atmospheric particles: A review of observations. *J. Aerosol Sci.* 35: 143–176.

- Kulmala M., Laakso L., Lehtinen K.E.J., Riipinen I., Dal Maso M., Anttila T., Kerminen V.-M., Hörrak U., Vana M. & Tammet H. 2004b. Initial steps of aerosol growth. *Atmos. Chem. Phys.* 4: 2553–2560.
- Kulmala M., Lehtinen K.E.J., Laakso L., Mordas G. & Hämeri K. 2005. On the existence of neutral atmospheric clusters. *Boreal Env. Res.* 10: 79–87.
- Kulmala M., Lehtinen K.E.J. & Laaksonen A. 2006. Cluster activation theory as an explanation of the linear dependence between formation rate of 3 nm particles and sulphuric acid concentration. *Atmos. Chem. Phys.* 6: 315–327.
- Kulmala M. & Tammet H. 2007. Finnish–Estonian air ion and aerosol workshops. *Boreal Env. Res.* 12: 237–245.
- Laakso L., Mäkelä J.M., Pirjola L. & Kulmala M. 2002. Model studies on ion-induced nucleation in the atmosphere. *J. Geophys. Res.* 107(D20), 4427, doi:10.1029/2002JD002140.
- Laakso L., Petäjä T., Lehtinen K., Kulmala M., Paatero J., Hörrak U., Tammet H. & Joutsensaari J. 2004. Ion production rate in boreal forest based on ion, particle and radiation measurements. *Atmos. Chem. Phys.* 4: 1933–1943.
- Laakso L., Grönholm T., Kulmala L., Haapanala S., Hirsikko A., Lovejoy E.R., Kazil J., Kurtén T., Boy M., Nilsson E.D., Sogachev A., Riipinen I., Stratmann F. & Kulmala M. 2007. Hot-air balloon measurements of vertical variation of boundary layer new particle formation. *Boreal Env. Res.* 12: 279–294.
- Lemmetty M., Marjamäki M. & Keskinen J. 2005. The ELPI response and data reduction II: properties of kernel and data inversion. *Aerosol Sci. Technol.* 39: 583–595.
- Likens G.E., Driscoll C.T. & Buso D.C. 1996. Long-term effects of acid rain: response and recovery of a forest ecosystem. *Science* 272: 244–246.
- Liu B.Y.H. & Pui D.Y.H. 1974. A submicron aerosol standard and the primary, absolute calibration of the condensation nuclei counter. *J. Coll. Interface Sci.* 47: 155–171.
- Lohmann U. & Feichter J. 2005. Global indirect aerosol effects: a review. *Atmos. Chem. Phys.* 5: 715–737.
- Mirme A. 1987. About the calibration of the electrical aerosol spectrometer. *Acta et comm. Univ. Tartuensis* 755: 71–79.
- O'Dowd C.D., McFiggans G., Creasey D.J., Pirjola L., Hoell C., Smith M.H., Allan B.J., Plane J.M.C., Heard D.E., Lee J.D., Pilling M.J. & Kulmala M. 1999. On the photochemical production of new particles in the coastal boundary layer. *Geophys. Res. Lett.* 26: 1707–1710.
- Ramanathan V., Crutzen P.J., Kiehl J.T. & Rosenfeld D. 2001. Aerosols, climate, and the hydrological cycle. *Science* 294: 2119–2124.
- Rosell-Llompart J., Loscertales I.G., Bingham D. & Fernández de la Mora J. 1996. Sizing nanoparticles and ions with a short differential mobility analyzer. *J. Aerosol Sci.* 27: 695–719.
- Ruuskanen T.M., Aalto P.P., Hörrak U., Vana M., Mårtensson M., Yoon Y., Kaasik M., Keronen P., Nilsson D., O'Dowd C., Noppel M. & Kulmala M. 2004. Observations of particle formation events during LAPBIAT measurement campaign in Värriö field station. *Report Series in Aerosol Science* 68: 266–269.
- Scheibel H.G. & Porstendörfer J. 1983. Generation of mono-disperse Ag- and NaCl-aerosols with particle diameters between 2 and 300 nm. *J. Aerosol Sci.* 14: 113–126.
- Stolzenburg M.R. 1988. *An ultrafine aerosol size distribution system*. Ph.D. thesis. University of Minnesota, Minneapolis, MN.
- Tammet H. 1970. *The aspiration method for the determination of atmospheric-ion spectra*. Israel Program for Scientific Translations Ltd., Jerusalem.
- Tammet H. 1983. Calibration of an electrical aerosol granulometer using the distribution of collected particles. *Acta et comm. Univ. Tartuensis* 648: 52–58.
- Tammet H. 1995. Size and mobility of nanometer particles, clusters and ions. *J. Aerosol Sci.* 26: 459–475.
- Tammet H. 2006. Continuous scanning of the mobility and size distribution of charged clusters and nanometer particles in atmospheric air and the Balanced Scanning Mobility Analyzer BSMA. *Atmos. Res.* 82: 523–535.
- Tammet H. & Noppel M. 1992. Principles of the graduation of an electric aerosol granulometer. *Acta et comm. Univ. Tartuensis* 947: 116–124.
- Tammet H.F., Jakobson A.F. & Salm J.J. 1973. Multichannel automatic air ion spectrometer. *Acta et comm. Univ. Tartuensis* 320: 48–75. [In Russian with English abstract].
- Tammet H., Mirme A. & Tamm E. 2002. Electrical aerosol spectrometer of Tartu University. *Atmos. Res.* 62: 315–324.
- Tammet H., Miller F., Tamm E., Bernotas T., Mirme A. & Salm J. 1987. Apparatus and methods for the spectrometry of small air ions. *Acta et comm. Univ. Tartuensis* 755: 18–28. [In Russian with English abstract].
- Thomson J.J. & Rutherford E. 1896. On the passage of electricity through gases exposed to Röntgen rays. *Philos. Mag.* 72: 392–407.
- Tikhonov A.N. 1963. Solution of incorrectly formulated problem and the regularization method. *Soviet Math. Dokl.* 4: 1035–1038.
- Vana M., Tamm E., Hörrak U., Mirme A., Tammet H., Laakso L., Aalto P.P. & Kulmala M. 2006a. Charging state of atmospheric nanoparticles during the nucleation burst events. *Atm. Res.* 82: 536–546.
- Vana M., Hirsikko A., Tamm E., Aalto P.P., Kulmala M., Verheggen B., Cozic J., Weingartner E. & Baltensperger U. 2006b. Characteristics of air ions and aerosol particles at the high-alpine research station Jungfraujoch. In: Biswas P., Chen D.-R. & Hering S. (eds.), *Proceeding of the seventh International Aerosol Conference*, St. Paul, Minnesota, U.S.A., 10–15 September, 2006, p. 1427.
- Virkkula A., Vana M., Hirsikko A., Aalto P.P., Kulmala M. & Hillamo R. 2005. Air ion mobility and aerosol particle size distributions in the marine boundary layer between Europe and Antarctica. In: Maenhaut W. (ed.), *Abstracts of the European Aerosol Conference 2005*, Ghent, Belgium, 28 August–2 September 2005, p. 651.
- Virkkula A., Hirsikko A., Vana M., Aalto P.P., Hillamo R. & Kulmala M. 2007. Charged particle size distributions and analysis of particle formation events at the Finnish Antarctic research station Aboa. *Boreal Env. Res.* 12: 397–408.

- Wang S.C. & Flagan R.C. 1990. Scanning electrical mobility spectrometer. *Aeros. Sci. Technol.* 13: 230–240.
- Whitby K.T. & Clark W.E. 1966. Electrical aerosol particle counting and size distribution measuring system for the 0.015 to 1.0  $\mu\text{m}$  size range. *Tellus* 13: 573–586.
- Yu F. & Turco R.P. 2001. From molecular clusters to nanoparticles: Role of ambient ionization in tropospheric aerosol formation. *J. Geophys. Res.* 106: 4797–4814.